

## ADVANCES IN AMELIORATING RHEUMATOID ARTHRITIS BY ANDROGRAPHOLIDE ETHOSOME-BASED GEL: PHARMACOKINETIC AND ACTIVITY STUDY IN RATS

KARTIKA FIDI ASTUTI<sup>1</sup> , SILVIA SURINI<sup>1\*</sup> , ANTON BAHTIAR<sup>2</sup> 

<sup>1</sup>Laboratory of Pharmaceutics and Pharmaceutical Technology, Faculty of Pharmacy, Universitas Indonesia, Depok, West Java, 16424, Indonesia, <sup>2</sup>Laboratory of Pharmacology and Toxicology, Faculty of Pharmacy, Universitas Indonesia, Depok, West Java, 16424, Indonesia  
Email: silvia@farmasi.ui.ac.id

Received: 15 Sep 2022, Revised and Accepted: 11 Nov 2022

### ABSTRACT

**Objective:** Andrographolide is the primary active constituent that was isolated from *Andrographis paniculata* and has been adopted to treat rheumatoid arthritis. Several studies revealed that it has poor oral bioavailability and skin penetration, which can be solved through the transdermal delivery of ethosomes. Therefore, this study aims to determine the pharmacokinetic profiles, relative bioavailability, and efficacy of andrographolide in the form of transdermal ethosomal gel in rheumatoid arthritis (RA) animal models.

**Methods:** Andrographolide was processed into ethosomes using the thin layer hydration-sonication technique. Its physical properties were then characterized, including particle size, polydispersity index, zeta potential, and entrapment efficiency, before it was incorporated into a gel dosage form. An *in vivo* study was also carried out on male *Sprague Dawley* rats. Subsequently, two gels, namely ethosomal and non-ethosomal, as well as an oral solution were prepared for the pharmacokinetic study. For the anti-rheumatic activity, thirty-six male rats were divided into three controls as well as three treatment groups, which were treated with 25, 50, and 100 mg/kg of andrographolide. During the induction and post-treatment phases, clinical manifestations of arthritis were thoroughly monitored.

**Results:** The andrographolide ethosomes were successfully prepared with particle sizes of  $76.35 \pm 0.74$  nm and entrapment efficiency of  $97.87 \pm 0.23\%$ . Based on the pharmacokinetic studies, the  $C_{max}$  obtained for ethosomal and non-ethosomal gel, as well as oral suspension, were  $53.07 \pm 4.73$ ,  $27.34 \pm 1.48$ , and  $11.72 \pm 0.74$   $\mu\text{g/ml}$  with  $AUC_{0-\infty}$  of  $152.10 \pm 16.53$ ,  $77.15 \pm 12.28$ , and  $23.20 \pm 3.46$   $\mu\text{g} \cdot \text{h/ml}$ , respectively. Furthermore, the relative bioavailability recorded for the preparations was 655.60%. Anti-rheumatic activity investigations revealed that the 50 and 100 mg/kg ethosomal gels reduced oedema volume closely with 0.135 mg methotrexate subcutaneously.

**Conclusion:** The ethosomal gel enhanced  $C_{max}$ ,  $AUC_{0-\infty}$ , and the relative bioavailability of andrographolide. Furthermore, it reduced oedema volume, ankle joint diameter, and arthritic scores in RA rats.

**Keywords:** Andrographolide, Ethosomes, Transdermal, Pharmacokinetic study, Rheumatoid arthritis

© 2023 The Authors. Published by Innovare Academic Sciences Pvt Ltd. This is an open access article under the CC BY license (<https://creativecommons.org/licenses/by/4.0/>)  
DOI: <https://dx.doi.org/10.22159/ijap.2023v15i1.46350>. Journal homepage: <https://innovareacademics.in/journals/index.php/ijap>

### INTRODUCTION

*Andrographis paniculata*, also known as sambiloto is one of the medicinal plants used in Indonesia and its major active constituent is andrographolide. The therapeutic effects of this component include action against rheumatoid arthritis and other chronic inflammatory disorders [1–3]. In mice with collagen-induced arthritis, Li *et al.* [4] revealed that oral suspension of 100 mg/kg BW andrographolide reduced the severity of the condition and joint destruction. Several studies have also explored its antiproliferation and pro-apoptotic activities on rheumatoid arthritis fibroblast-like synoviocyte cells (RAFLS), which have anti-inflammatory properties [5].

A diterpenoid substance identified as andrographolide has a log *P* value of 2.632 and a solubility of 3.29  $\mu\text{g/ml}$  at 25 °C [6]. Furthermore, it has an oral bioavailability of 2.67% in rats with a 120 mg/kg BW dose [7, 8]. It is often metabolized by the duodenum and jejunum into hydrophilic and impermeable sulphate metabolites. Several studies revealed that andrographolide has a low oral availability due to poor water solubility as well as the presence of efflux transporters, which tend to pump it back into the gut lumen [7]. Approximately 55% of andrographolides administered orally are excreted through the bile [9]. These findings showed that its solubility and bioavailability are likely to be a challenge for further study; hence, the dosage form is expected to address this laxity.

Transdermal drug delivery is an alternative approach adopted to enhance the bioavailability of andrographolide by avoiding the hepatic first-pass metabolism, drug degradation, and gastrointestinal efflux pump [10, 11]. This approach also lessens patient pain because there is no requirement for oral administration due to its unpleasant taste [12]. However, this bioavailability is limited by the stratum corneum, which is the main barrier to therapeutic penetration through the skin [13].

Several forms of lipid nanovesicles can be used as drug carrier systems to improve penetration through the skin [14]. Ethosomes are used for transdermal delivery because they enable drugs to penetrate the skin more easily into the systemic circulation due to their elasticity and flexibility compared to liposomes [15]. Their high alcohol content tends to disorganize and alter the permeability of the stratum corneum's lipid bilayer structure, thereby enhancing transdermal penetration [16]. A recent study by Martihandini *et al.* [17] revealed that andrographolide encapsulated on ethosome has a vesicle size range of 92.27–123.00 nm, zeta potential  $> \pm 30$  mV, and entrapment efficiency of 97.10%–97.93%. The results also revealed that there was an improvement in skin penetration. Findings showed that no study has not provided *in vivo* test data on the pharmacokinetic profile and anti-rheumatic activity of andrographolide ethosome-based gel. Therefore, this study aims to evaluate the pharmacokinetic and anti-rheumatoid arthritis activity of andrographolide ethosome-based gel (AEG) in rats using transdermal administration.

### MATERIALS AND METHODS

#### Materials

The materials used in this study include andrographolide powder (purity 99%) purchased from Shaanxi Hongda Phytochemistry Co. (Shanghai, China), and standard andrographolide from Sigma Aldrich (Singapore). Furthermore, phospholipon 90 G was purchased from Lipoid (Nattermannallee, Germany). Laboratory-grade ethanol, hydroxy propyl methyl cellulose (HPMC), propylene glycol, methanol, methylparaben, propylparaben, potassium phosphate monobasic, sodium hydroxide, and acetone were acquired from Merck (Darmstadt, Germany). Complete Freund's Adjuvant (CFA) was obtained from Sigma Aldrich (Singapore), while

a methotrexate injection 25 mg/ml was purchased from PT CKD OTTO Pharmaceuticals (Bekasi, Indonesia).

### Experimental animals

The experiment was carried out on male white rats (*Rattus norvegicus*) Sprague Dawley aged 2-3 mo and weighing 175-300 grams. The test animals were obtained from Bogor Agricultural University, Bogor, Indonesia. Furthermore, one cage consisted of six rats kept at a room temperature of  $25 \pm 2$  °C and 60-70% humidity with a twelve-hour day/night cycle. All the test animals were provided with adequate food and water. The experimental protocol was approved by the Ethical Committee of Cipto Mangunkusumo Hospital, Faculty of Medicine, Universitas Indonesia, with Registration Number KET-417/UN2. F1/ETIK/PPM.00.02/2022.

### Preparation of andrographolide ethosome-based gel

The ethosomal suspension containing andrographolides and phospholipids with a weight ratio of 1:9, w/w was prepared using the thin layer hydration method, as proposed by Martihandini *et al.* [17]. Subsequently, it was formulated into a gel preparation containing 10 mg andrographolides/g gel, and another sample was prepared without ethosomes for comparison.

### Characterization of andrographolide ethosome-based gel

The ethosomes obtained were assessed for their particle size, polydispersity index (PDI), and zeta potential using a computerized Particle Size Analyzer (PSA) Zetasizer ZS90 (Malvern, UK). Furthermore, the entrapment efficiency was determined with a direct method by taking pellets containing andrographolides trapped in the lipid matrix, which was collected after centrifuging solid lipids from the dispersion medium. The andrographolide ethosome-based gel was then evaluated for its homogeneity, pH level, viscosity, as well as organoleptic and rheology properties.

### In vivo pharmacokinetic study

The thirty-six animals were divided equally into three groups and then subdivided into two smaller groups (n=6). Blood samples were also serially from the rats at various intervals. In this study, 50 mg/kg BW andrographolide was administered in three different formulations, namely ethosome-based gel (AEG), non-ethosome-based gel (ANEG), and oral suspension (AOS). Furthermore, transdermal administration of AEG and ANEG was carried out in the abdomen region of the rats.

Blood samples were collected from the retro-orbital plexus at intervals of 0, 0.5, 1, 2, 3, 4, 6, 8, 12, and 24 h. They were then placed in an Eppendorf tube with sodium tripotassium ethylenediaminetetraacetic acid (EDTA) as an anticoagulant. Samples at 0, 0.5, 1, 2, and 3 h were taken from subgroup (a), while those at 4, 6, 8, 12, and 24 h were collected from subgroup (b). Replacement of isotonic fluid was used to prevent blood deficiency in experimental animals after repeated sampling by injecting a saline solution, namely 0.9% sodium chloride, intraperitoneally 3-4 times.

Plasma from blood samples was transferred to microtubes and kept at -80 °C after centrifugation at 3,000 rpm and 4 °C for 15 min. Subsequently, 200 µl of plasma and 4 ml of acetone were combined, and the mixture was vortexed for two minutes. Protein was precipitated at 4 °C for 5 min, followed by centrifugation at 3,000 rpm at room temperature for 15 min. The supernatant was evaporated with a vacuum evaporator, while the residual material was dissolved in 100 µl of methanol before being centrifuged at 3,000 rpm for 15 min. High-Performance Liquid Chromatography (HPLC) analysis was then used to determine the concentration of andrographolide in the plasma samples [18, 19].

Andrographolide concentration in the plasma was assessed with the reverse-phase HPLC after extraction using reported assays [19] with modifications. The HPLC system Shimadzu's (Japan's) has a UV detector, the Zorbax Eclipse Plus C18 column (250 x 4.6 mm, 5 µm particle) was used for separation, and the mobile phase consisted of methanol and water in a ratio of 60:40 at room temperature and flow rate of 0.8 ml/min. The injection volume used was 20 µl, while the effluent was observed at 225 nm. Various pharmacokinetic

parameters, including  $C_{max}$  and  $T_{max}$ , were determined directly from the graph curve of plasma drug concentration against time. The trapezoidal log-linear rule determines the area under the curve ( $AUC_{0-\infty}$ ). Furthermore, the slope of the log plasma concentration against the time plot was used to compute the first-order elimination rate constant ( $k_e$ ), while the elimination half-life ( $t_{1/2}$ ) was estimated using the formula  $t_{1/2} = 0.693/k_e$ . The relative bioavailability (F) of andrographolide after transdermal administration was calculated using the equation below:

$$F = \frac{AUC_{0-\infty} (\text{sample, transdermal})}{AUC_{0-\infty} (\text{reference, oral})} \times 100\%$$

The standard andrographolide stock solution was prepared at a concentration of 1 mg/ml, followed by sonication for ten minutes at room temperature. Blood plasma was used to dilute the solution to a concentration of 60.6 µg/ml-0.0095 µg/ml. Subsequently, 2 ml of acetone was added to the mixture and vortexed for two minutes. The plasma was then centrifuged for 30 min at 3,000 rpm. Reverse phase HPLC was used to evaluate the supernatant obtained.

### In vivo anti-rheumatoid arthritis activity study

#### Animal preparation

All the animals were handled gently for two weeks, and their body weights were recorded periodically. They were then divided into Complete Freund's Adjuvant (CFA) induced (five groups; n=30) and control (one group; n=6) rats. Each group contained six rats, namely:

- Group 1 = Normal control, which received 0.1 ml of saline solution on the first day (induction phase), and for a total of 21 d. Subsequently, 1 g of ethosomal gel base was administered transdermally in the abdomen of the rats.
- Group 2 = Negative control received a subplantar injections of 0.1 ml CFA on the first day (induction phase) on their right hind paws and monitored for 14 d. They were then administered with 1 g of gel base transdermally in the abdomen for 21 d.
- Group 3 = Positive control received a subplantar injection of 0.1 ml CFA for the first day and monitored for 14 d (induction phase) before receiving a dosage of 0.135 mg methotrexate per quarter per week subcutaneously for 21 d.
- Group 4 = received subplantar injections of 0.1 ml CFA on the first day (induction phase) and monitored for 14 d. They were given a dosage of 25 mg/kg AEG for 21 d transdermally in the abdomen.
- Group 5 = received subplantar injections of 0.1 ml CFA on the first day (induction phase) and monitored for 14 d. They were then administered with a dosage of 50 mg/kg AEG for 21 d transdermally in the abdomen.
- Group 6 = received subplantar injections of 0.1 ml CFA on the first day (induction phase) and monitored for 14 d. They were then given 100 mg/kg AEG for 21 d transdermally in the abdomen.

#### Induction of arthritis

The rheumatoid arthritis was induced in overnight-fasted rats with a single subplantar injection of 0.1 ml CFA under 50 mg/kg BW ketamine anaesthesia using a single intraperitoneal injection. A group of non-arthritic age-matched rats received an equal volume of saline, namely 0.1 ml, and were used as the controls. The incidence of arthritis as assessed from the scoring and based on the preliminary study was 100% (30/30 immunized rats). In this study, rheumatoid arthritis was induced with 0.1 ml CFA on the first day and monitored for 14 d. The occurrence of the condition was confirmed with the criterion that the volume of paw oedema >0.04 ml, the ankle joint diameter >4.5 mm, and the arthritis score was >1 after induction [20-22].

#### Treatment and assessment of clinical signs of rheumatoid arthritis

On the 15th day after subplantar CFA induction, the treatment administration was carried out for 21 d on the rats. The test animals were weighed and monitored for clinical signs of arthritis after

induction every 2 d until day 14. The clinical scoring system was employed as follows: there was no inflammation in the finger scores 0 (no arthritis), 0.25-swollen and redness on one toe, 0.5-swollen and redness in at least two toes, 0.75-swelling of the soles of the feet, 1.00-swelling and redness of the toes and changes in the shape of the feet's soles, 1.25-swelling and redness of the toes and soles of the feet, 1.5-swelling and redness of the toes, as well as slight swelling in the soles and ankles, 1.75-swelling and redness of the fingers, with a swelling of most of the soles and ankles, and 2.00-swelling and redness of the toes, soles, and ankles [22].

The scoring was tripled with the measurement of ankle joint diameter and oedema volume because it can only provide a subjective qualification of inflammation. Observation of the anti-rheumatic effect was indicated by the reduction in the ankle joint diameter in the hind paws of the test rats, as measured by a digital caliper. It was also indicated by a decrease in the volume of oedema by 50% on day 21 after treatment with andrographolide ethosomes on the hind paw, and this was measured using a plethysmometer. The rat paws' volume, ankle joint diameter, and arthritic scores were measured before the injection of 0.1 ml CFA. After the treatment, this procedure was repeated on days 1, 3, 5, 7, 10, 14, and 21.

The data of the anti-rheumatic activity study were obtained from the diameter of the hind paws, the volume of oedema, and the percentage of average inhibition of oedema. Furthermore, each group of rats was observed on the arthritis index based on the incidence score to evaluate the progression and severity of the condition. The result obtained for the andrographolide-treated and positive control group were compared with the normal and negative control.

#### Statistical analysis

The plasma levels of andrographolide and the pharmacokinetic characteristics of the treatment groups were compared using a t-test. The anti-arthritis activity was then examined using Saphiro-Wilk to check whether the data were normal, while Levene's test was used to determine data homogeneity. Furthermore, to determine the differences between each treatment group, an analysis of variance test (ANOVA) with a 95% confidence level was performed on the data if they were normally distributed and homogenous. This was followed by the Least Significant Difference (LSD) test. If the data are not homogeneous and normally distributed, the Kruskal-Wallis test was used to determine the difference. The Mann-Whitney test determined the disparity between each treatment group when there was a significant difference. Data analysis was carried out using the IBM SPSS Statistics 25.

## RESULTS

### Characterization of andrographolide ethosome-based gel

In this study, ethosomes size ranged from 75.50 to 77.60 nm based on the findings. Furthermore, the formulas' PDI was less than 0.3, and the zeta potential values were determined in triplicate using the same tool, namely  $> \pm 30$  mV. The detailed result of this characterization is presented in table 1. The direct method yielded an entrapment efficiency of  $97.87 \pm 0.23$  % in the andrographolide ethosomes formula.

The andrographolide ethosome-based gel was evaluated and it was white in color, while the non-ethosomal variant was pale white. Furthermore, the formula appeared homogeneous when spread on a glass slide, with no visible coarse particles. The pH of the ethosomal gels was within the skin's acceptable range of 4.5-6.5. In this study, the viscosity of the sample was measured using a Cole Parmer VCPL 100008 rotational viscometer with an L4 spindle. The results showed that AEG had a higher viscosity than ANEG. The rheology evaluation revealed that all formulas had a thixotropy plastic flow, as shown in fig. 1.

### Pharmacokinetic study

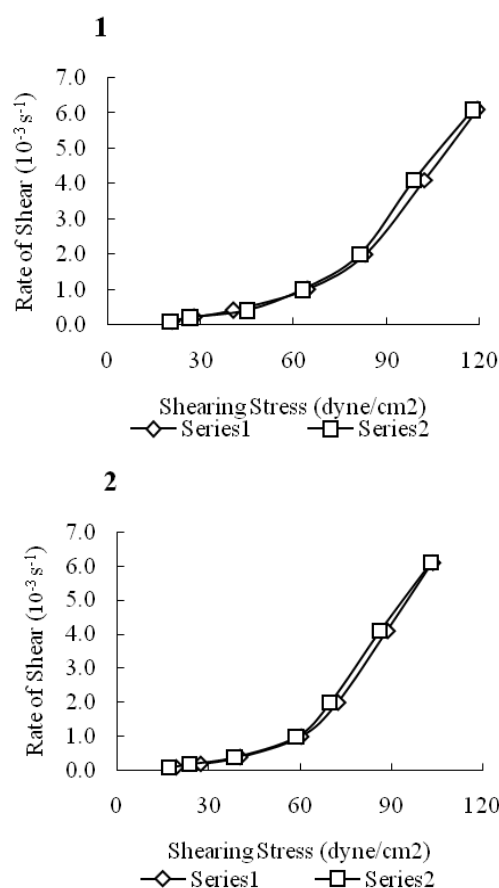
Table 2 shows the pharmacokinetic study results, while the mean plasma concentration-time profile of andrographolide in rat plasma

after transdermal and oral administration at 50 mg/kg body weight is presented in fig. 2. After the transdermal administration of AEG and ANEG, initial drug concentrations of  $0.23 \pm 0.02$   $\mu\text{g/ml}$  and  $0.04 \pm 0.03$   $\mu\text{g/ml}$  were observed at 0.5 h, respectively. At 6 h, the mean peak plasma concentration of AEG was  $53.07 \pm 4.73$   $\mu\text{g/ml}$ , which quickly dropped to  $0.79 \pm 0.02$   $\mu\text{g/ml}$ , while ANEG was  $27.34 \pm 1.48$   $\mu\text{g/ml}$  and it decreased significantly to  $0.05 \pm 0.17$  at 24 h. Meanwhile, 8 h after the oral administration of AOS, the level in the plasma was  $0.04 \pm 0.03$   $\mu\text{g/ml}$ , and the drug was not detectable afterward.

**Table 1: Andrographolide ethosomes characterization**

Parameters	Average $\pm$ SD
Dv 10 (nm)	23.27 $\pm$ 3.61
Dv 50 (nm)	36.17 $\pm$ 2.05
Dv 90 (nm)	76.7 $\pm$ 1.08
Dv mean (nm)	46.54 $\pm$ 2.94
Z-avg (nm)	76.35 $\pm$ 0.74
Polydispersity index	0.26 $\pm$ 0.01
Zeta potential (mV)	-40.17 $\pm$ 1.03

All value were represented as the mean $\pm$ SD (n=3)



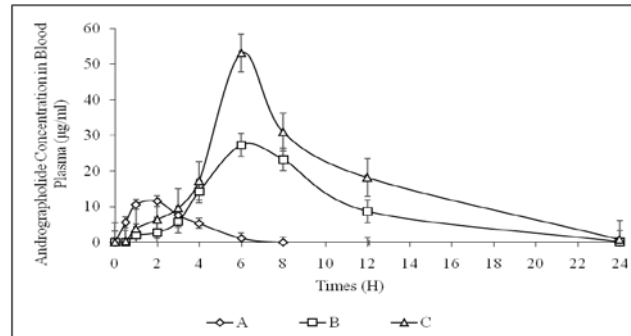
**Fig. 1: The rheogram of andrographolide-loaded ethosomal and non-ethosomal gel; 1: rheology of AEG. 2: rheology of ANEG**

Table 2 showed that the half-time ( $t_{1/2}$ ) and half-time absorptions ( $t_{1/2abs}$ ) of AEG were longer than those of ANEG and AOS. The pharmacokinetic study found that  $k_e$  for AEG was lower than ANEG despite having similar  $t_{max}$ . The relative bioavailability of the transdermal formula was also determined using a pharmacokinetic study. Based on the calculation of the  $AUC_{0-\infty}$  ratio between the transdermal and oral routes, the bioavailability of the AEG and ANEG was 655.60% and 332.54%, respectively.

**Table 2: Pharmacokinetic parameters from the pharmacokinetic study**

Parameters	AEG	ANEG	AOS
$C_{max}$ ( $\mu\text{g}/\text{ml}$ )	53.07 $\pm$ 4.73	27.34 $\pm$ 1.48	11.72 $\pm$ 0.74
$t_{max}$ (h)	6.00 $\pm$ 0.00	6.00 $\pm$ 0.00	2.00 $\pm$ 0.00
AUC <sub>0-<math>\infty</math></sub> ( $\mu\text{g}\cdot\text{h}/\text{ml}$ )	152.10 $\pm$ 16.53	77.15 $\pm$ 12.28	23.20 $\pm$ 3.46
$k_e$ (/h)	0.24 $\pm$ 0.01	0.25 $\pm$ 0.05	1.11 $\pm$ 0.12
$t_{1/2}$ (h)	2.94 $\pm$ 0.06	2.75 $\pm$ 0.47	0.63 $\pm$ 0.09
$t_{1/2}$ absorption (h)	2.41 $\pm$ 0.06	2.38 $\pm$ 0.43	0.55 $\pm$ 0.04

AEG: andrographolide ethosome-based gel; ANEG: andrographolide non-ethosome-based gel; AOS: oral suspension of andrographolide. All value were represented as mean $\pm$ SD (n=6)



**Fig. 2: Plasma concentration-time profiles of andrographolide in rats after single transdermal administration of 50 mg/kg andrographolide. Each point represents the mean $\pm$ SD, n=6. A: oral suspension of andrographolide (AOS), B: andrographolide non-ethosome-based gel (ANEG), C: andrographolide ethosome-based gel (AEG)**

### Anti-rheumatoid arthritis activity study

#### Effect on ankle joint swelling

Andrographolide ethosome-based gel treatments significantly relieved joint oedema in CFA-induced arthritis rats, as shown in fig. 3. The swelling was evaluated using the ankle joint diameter, oedema volume, and arthritis scores for 21 d of treatment.

Based on the results, there was no obvious swelling paw in the control group during the induction time. Meanwhile, in the negative control, adjuvant-induced arthritis resulted paw oedema 0.073 ml on day 9 and ankle joint diameter increased from 2.37 mm on day 0 to 7.33 mm after 9 d of induction. The arthritic scores also increased from 0 on day 0 to 2 on day 12.

After administering 0.135 mg methotrexate subcutaneous injection, the positive group showed a significant decrease in these three parameters. Treatment with andrographolide ethosome-based gel in graded doses, namely 25, 50, and 100 mg/kg BW administered transdermally, showed a significant reduction of the ankle joint diameter, oedema volume, and arthritic scores compared to the negative control, which received a gel base. Among the other doses, 25 mg/kg BW AEG gave the slightest decrease. Meanwhile, the group that received a dose of 50 mg/kg BW showed a decrease that was almost the same as that of the 100 mg/kg BW dosage, though it provided a more effective reduction at the beginning of the administration.

#### Percentage of oedema inhibition

Table 4 and fig. 3 (4) showed that one day after the treatment, the positive control had a large percentage of oedema inhibition, namely 35.42%, while a lower value was recorded in the AEG treatment group. Furthermore, AEG at a dose of 50 mg/kg inhibited the largest amount of oedema, followed by the 25 mg/kg and 100 mg/kg dosages. However, from day 3 to day 21, the 100 mg/kg group showed a more significant inhibition percentage than 25 mg/kg. Based on these findings, ethosomal andrographolide gel effectively reduced oedema in arthritic rats.

Apart from the dosage of 25 mg/kg, other groups administered with different doses of AEG showed outcomes that were close to the normal control on day 21. This finding indicates that the experimental rats have recovered from chronic arthritis. Furthermore, AEG doses of 50 mg/kg and 100 mg/kg produced outcomes that were similar to the positive control given 0.135 mg methotrexate subcutaneous injection. The group receiving 25 mg/kg showed the lowest oedema inhibition. Based on these findings, andrographolide ethosome-based gel doses of 50 mg/kg and 100 mg/kg had a similar inhibitory effect on oedema with the positive control, namely > 70% inhibition 21 d after treatment. However, the inhibitory response was faster in the positive control, while the 25 mg/kg dose had the lowest effect and needed a longer time to function compared to 50 and 100 mg/kg AEG.

**Table 3: Clinical signs of rheumatoid arthritis in rats after drug treatment for 21 d**

Group	Clinical signs	Post-treatment (day)							
		0	1	3	5	7	10	14	21
Normal control	V	0.020	0.020	0.021	0.021	0.021	0.021	0.021	0.021
	D	2.20	2.23	2.23	2.27	2.270	2.270	2.270	2.230
Negative control	V	0.066	0.064	0.060	0.057	0.053	0.049	0.042	0.034
	D	6.70	6.42	6.13	5.70	5.38	5.00	4.47	3.40
Positive control	V	0.057	0.050	0.044	0.042	0.039	0.036	0.033	0.025
	D	5.70	5.03	4.35	3.97	3.87	3.60	3.32	2.60
AEG 25 mg/kg BW	V	0.060	0.054	0.050	0.045	0.043	0.039	0.035	0.029
	D	6.03	5.45	5.03	4.50	4.30	4.00	3.62	3.23
AEG 50 mg/kg BW	V	0.060	0.051	0.044	0.041	0.039	0.036	0.032	0.026
	D	6.03	4.87	4.03	3.52	3.38	3.23	2.95	2.57
AEG 100 mg/kg BW	V	0.063	0.056	0.050	0.043	0.041	0.038	0.033	0.027
	D	6.32	5.58	5.02	4.60	4.28	3.87	3.35	2.67

V: oedema volume (ml), D: ankle joint diameter (mm). Data are presented as average (n=6)

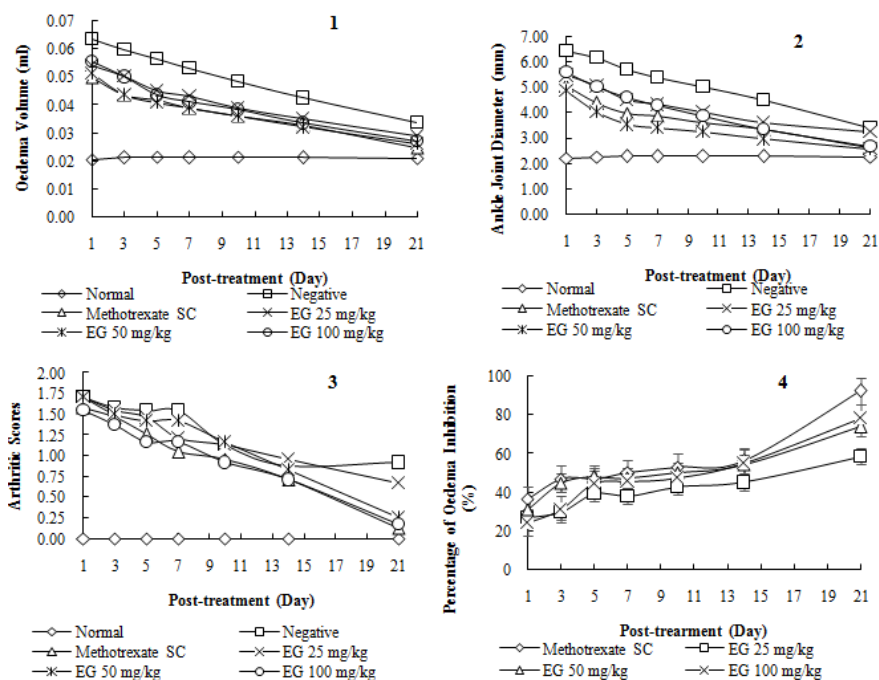


Fig. 3: Clinical signs of rheumatoid arthritis; 1: oedema volume post-treatment, 2: ankle joint diameter post-treatment, 3: arthritic scores post-treatment, 4: percentage of oedema inhibition post-treatment. Data are presented as the means $\pm$ SD (n=6)

Table 4: Percentage of oedema inhibition in the treatment group of rats for 21 d

Group	Percentage of oedema inhibition (%) after drug treatment						
	Day 1	Day 3	Day 5	Day 7	Day 10	Day 14	Day 21
Methotrexate 0.135 mg	35.42	46.19	46.76	51.52	53.02	56.11	92.45
AEG 25 mg/kg	25.85	29.50	38.22	36.97	41.76	44.64	55.16
AEG 50 mg/kg	29.84	43.79	46.41	47.51	48.81	53.31	71.83
AEG 100 mg/kg	22.13	30.46	44.27	44.02	46.56	54.53	77.31

Data are presented as average (n=6).

## DISCUSSION

The development of the AEG formula has been previously carried out by Martihandini *et al.* [17], where andrographolides formulated in ethosomes with an andrographolide-phospholipid ratio of 1:9 increased drug penetration through the skin using transdermal delivery in an *in vitro* study. Therefore, in this study, the formula and method of preparation as well as characterization was performed based on the method in Martihandini *et al.* [17].

This study also incorporated andrographolide into ethosomes formulation at a concentration of 1%. Vesicle size is essential in transdermal drug delivery using the ethosomes formula. The dynamic light scattering (DLS) approach yielded vesicle size measurements of less than 300 nm. The PDI value was generated when the sizing was determined using DLS, and this is consistent with Martihandini *et al.* [17]. This value indicates the degree of heterogeneity in a dispersed system based on the particle. The PDI was less than 0.3, indicating that the size distribution was uniform [23]. The zeta potential value was interpreted as electrical repulsion, which prevents particle aggregation, thereby leading to a dispersed system with good stability [24]. The pH of the hydration solution led to the occurrence of negative zeta potential in the ethosomes.

Based on the results, the EE (%) values of the andrographolide ethosomes were greater than 97%, and this is consistent with the previous study on the EG2 formula [17]. Increasing the phospholipid concentration tends to enhance the size and strength of the vesicle membrane, thereby leading to an increased number of entrapped drugs [23, 25]. Andrographolide is a lipophilic substance enclosed in the lipid bilayer of the vesicle, and this indicates that increasing the

phospholipid helps to improve the entrapment efficiency [17]. This result is supported by a prior study that formulated bitter melon in ethosomes, resulting in entrapment efficiency of 83.85-92.65%, which improved skin penetration [26]. When compared to transfersomes in the research of Surini *et al.* [27], who formulated recombinant human epidermal growth factor in transfersomal emulgel, the resultant entrapment efficiency was 97.77 $\pm$ 0.09%. This demonstrates that encapsulating drugs in lipid vesicles can improve entrapment efficiency and penetration through the skin.

The ethosomes were integrated into the gel in this study to make the system more suitable for transdermal application, with HPMC as a gelling agent. Furthermore, the viscosity of the preparation is essential for facilitating application on the skin and controlling the drug release profile [28].

The results of the pharmacokinetic studies correspond to the results of the *in vitro* penetration experiments. Based on data from *in vitro* test reported by Marthandini *et al.* [17], the flux in AEG formulations was greater, at 5.16 $\pm$ 0.10  $\mu$ g/cm<sup>2</sup>/hour, than in ANEG, which was 1.77 $\pm$ 0.03  $\mu$ g/cm<sup>2</sup>/hour. These findings were confirmed by data on AUC<sub>0-∞</sub> values in *in vivo* evaluation in this research, which showed that AEG preparations have a higher AUC<sub>0-∞</sub> than ANEG. The elevation in AUC<sub>0-∞</sub> value is connected to the characteristics of the obtained ethosomes, particularly particle size. The smaller the drug particle, the greater its penetration and plasma concentration. These data suggest that ethosomes can enhance andrographolide penetration and plasma concentrations.

Based on the pharmacokinetic investigation, there were substantial differences in the AUC<sub>0-∞</sub> of AEG compared to ANEG and OS (P<0.05).

The area under the curve,  $AUC_{0-\infty}$  represents the drug levels in the systemic circulation against time. It also describes the degree of absorption, namely the medication absorbed from a given dose. The area under the concentration-time curve can be used to calculate the number of unchanged drugs that reached systemic circulation [29, 30]. Fig. 2 demonstrates that  $AUC_{0-\infty}$  values in AEG preparations are twice as high as in ANEG. Furthermore, as compared to AOS, the  $AUC_{0-\infty}$  value in AEG increased by over six times. The increase in  $AUC_{0-\infty}$  value was achieved by entrapping andrographolide into the ethosomes. As a result, drug penetration into the skin increased, increasing the amount of drug in the systemic circulation over time [27].

$C_{max}$  and  $t_{max}$  are two additional pharmacokinetic parameters. The highest concentration of andrographolide in plasma ( $\mu\text{g/ml}$ ) is represented by  $C_{max}$ , while the time required to reach peak levels is represented by  $t_{max}$  (hour).  $C_{max}$  in AEG increased dramatically, twice as much as in ANEG and almost five times as much as in AOS. The  $t_{max}$  value achieved by the same route, transdermally (AEG and ANEG), was the same at the sixth hour. In the meantime, when administered orally in AOS,  $t_{max}$  was reached earlier, in the second hour. These results demonstrate that transdermal delivery of ethosomes andrographolide improved  $C_{max}$  and  $t_{max}$ .

The value of  $t_{1/2}$  and  $t_{1/2\text{absorption}}$  represents the elimination and absorption half-life, respectively. The half-life of a drug is the time required to reduce its concentration in the body by half through elimination [29, 30]. The results also showed that AEG has a longer half-time than ANEG and AOS, which was directly proportional to the concentration of the drug in blood plasma. The higher the  $C_{max}$  of substances in circulation, the longer it takes the body to eliminate them. This finding is consistent with Pirvu *et al.*, [31] that it is beneficial in terms of dose and frequency of administration. These advantages can lead to better patient compliance, lower production costs, and fewer dose-related side effects [32].

The elimination rate constant ( $k_e$ ) indicates the fraction of a drug eliminated in one unit of time. It is also the rate at which the therapeutic concentration declines once the kinetic process reaches equilibrium. The  $k_e$  for AEG was lower than ANEG, indicating that andrographolide released from AEG was removed slowly from the rat's blood. Based on the low  $k_e$ , AEG also has the potential to be used as a sustained-release dosage form. Meanwhile, the value of  $k_e$  in AOS formulations is higher, indicating that the drug is removed from the body's circulation more speedily. These findings supported by data of plasma drug quantification in oral suspension, where the drug was undetectable after 8 h.

The fraction of a drug delivered extra vascularily, which reached the systemic circulation is referred to as bioavailability. Furthermore, it is known as relative bioavailability when measured between two routes of administration, dosage type, or formulation [33]. These results indicated that transdermal delivery of andrographolide (AEG and ANEG) can provide better bioavailability compared to oral treatment. The oral bioavailability of the drug is low because it is rapidly metabolized by first-pass metabolism. Furthermore, andrographolide is converted into sulfonate (14-deoxy-12-sulfo-andrographolide) through enzymatic reaction or microorganisms, followed by glucuronidation, sulfation, or methylation [7]. This problem can be solved through the selection of a better delivery route.

The results showed that the bioavailability of andrographolide was greatly enhanced ( $P < 0.05$ ) by processing it into a transdermal ethosomal gel that achieved at value of 655.60% for AEG and 332.54% for ANEG. A previous study revealed that when it is taken orally, the drug is promptly metabolized. Andrographolide can be transported directly into circulation to all body regions after passing through the hepatic metabolism. This makes transdermal delivery an alternative method for increasing its bioavailability. A previous study revealed that entrapping drugs in submicron vesicles can enhance their bioavailability [34]. It has been demonstrated by *in vitro* penetration [17] that the deformability and flexibility of ethosomes to pass through the skin can improve andrographolide penetration. This can make its bioavailability significantly higher when compared to ANEG ( $P < 0.05$ ).

These anti-arthritis studies aim to collect data on the efficacy of ethosomal andrographolide transdermal formulations in rheumatoid arthritis animal models. Rheumatoid arthritis is an autoimmune disease characterized by inflammation, progressive bone erosion, and cartilage damage, leading to synovial hypertrophy [35]. Therefore, the CFA model, which is the most extensively studied autoimmune model of the condition, was produced in *Sprague Dawley* rats.

The results showed that andrographolide reduced arthritis by decreasing oedema volume, ankle joint diameter, and arthritic scores. This effect was related to its anti-inflammatory properties. Modulation of nuclear factor kappa B (NF- $\kappa$ B) binding to deoxyribonucleic acid (DNA) suppresses the expression of proinflammatory proteins, such as cyclooxygenase 2 (COX-2) and nitric-oxide (NO) synthase [36]. Andrographolides contain an unsaturated- $\gamma$ -lactone structure that can form covalent interactions with nucleophilic sites in proteins, such as cysteine residues. A covalent connection between this compound and cysteine residue 62 (Cys-62) of p50, which is the major subunit of transcription factor NF- $\kappa$ B, reduces the transcriptional activity of NF- $\kappa$ B oligonucleotides in the nucleus. Cys-62 can be found in the p50 L1 loop, a DNA binding pocket [37].

Fig. 3 shows a decrease in oedema volume, ankle joint diameter, and arthritic scores in all arthritis rat groups, including the non-treatment group (negative control). It was because rats are mammals and can heal themselves spontaneously against diseases by consuming the food around them, thereby affecting self-medication. The experimental animals were fed with BR-12 containing 0.8 to 1.1% calcium, which is beneficial in treating rheumatoid arthritis. This is because it can reduce bone mineral density loss in the lumbar spine and trochanter [40]. However, further research is needed to understand its influence in meals on recovery from the condition. Moreover, there are some limitations in the animal models of rheumatoid arthritis induced by adjuvants, and they are related to the mechanism of the chronic progression of RA events as well as the pathological changes in test animals. It can also be explained molecularly that naturally occurring CD4+regulatory T (Treg) cells are characterized by constitutive expression of the transcription factor IL-2 receptor (CD25). Tregs maintain immunological tolerance and prevent autoimmune disease by suppressing the activation and proliferation of effector T cells. Dendritic cells (DCs) are professional antigen-presenting cells that instruct T cells, based on their surrounding environment, to mediate an immune response or tolerance [38].

Meanwhile, there was a substantial decrease in oedema volume and joint diameter in the positive control that received 0.135 mg methotrexate subcutaneous injection compared to the non-treatment and ethosomal gel treatment groups. Despite its moderate immunosuppressive and anti-inflammatory effects, methotrexate significantly reversed CFA-induced physiological, biochemical, and molecular alterations in arthritic rats. The treatment also elevated the levels of anti-inflammatory cytokine interleukin 10 (IL-10). Methotrexate significantly reduced synovial TNF- $\alpha$  levels, lowered synovial tumor necrosis factor  $\alpha$  (TNF- $\alpha$ ), and restored NO<sub>2</sub> levels to normal [39].

The treatment group that received AEG at three graded doses, namely 25, 50, and 100 mg/kg BW, showed a reduction in oedema volume and joint diameter. However, the results demonstrated that the 25 mg/kg BW dose resulted in the slightest decrease after 21 d of therapy. The ankle joint diameter remained elevated and will take some time to return to normal (around 2 mm). The group that received a dose of 50 mg/kg BW showed a drop in oedema volume and joint diameter that was similar to that of the 100 mg/kg BW. However, it provided a more effective reduction at the beginning of the administration.

Based on the percentage inhibition of oedema calculation results, the most significant percentage of oedema inhibition on the first day of treatment was shown with AEG at a dosage of 50 mg/kg, followed by 25 mg/kg and 100 mg/kg. The lower inhibitory value at 100 mg/kg AEG can be attributed to the delivery of  $\pm 2$  g of gel remaining in the ring. The attached ring was somewhat disengaged from the

attachment site, hence, all the drugs did not penetrate the skin layer and become properly absorbed. AEG doses of 50 mg/kg and 25 mg/kg can enter the epidermal layer, and only a little amount was left, hence, the oedema inhibitory action was more significant. From day 3 to day 21, the dosage of 50 and 100 mg/kg provided a more significant percentage of inhibition compared to the 25 mg/kg. The increased effect at 100 mg/kg was because the difficulty on the first day of treatment had been solved through the use of a better adhesive to avoid detachment of the ring.

According to the findings of the anti-arthritis experiments, the three doses assessed had positive effects on the activity test parameters after 21 d of treatment. At the dose of 50 mg/kg, it significantly decreased oedema volume and joint diameter as well as inhibited oedema volume by more than 70% in arthritic rats from to initial conditions, attempting to make 50 mg/kg the recommended dose of andrographolide for the treatment of rheumatoid arthritis. This dose suggestion considers the adverse effects, which are predicted to be mild at the moderate dose.

Data on these parameters for the tested group fulfilled the test requirements for normal and homogeneous distribution based on statistical analysis. This study was conducted to determine the feasibility of the data on the parametric test, particularly data from a normally distributed population with the same variance.

## CONCLUSION

Transdermal administration of the andrographolide ethosome-based gel elevated the  $C_{max}$  and  $AUC_{0-\infty}$  value compared to the non-ethosome-based gel and oral suspension of andrographolide. Furthermore, ethosomal gel provided greater relative bioavailability of andrographolide compared to non-ethosomal gel. Therefore, ethosomal gel is effectively useful to reduced oedema volume, ankle joint diameter, and arthritic scores in rheumatoid arthritis rats at the dose of 50 mg/kg.

## ACKNOWLEDGMENT

The authors gratefully acknowledge Ministry of Research and Technology/National Research and Innovation Agency for the research grant NKB-007/UN2. RST/HKP.05.0/2021.

## FUNDING

Nil

## AUTHORS CONTRIBUTIONS

KFA contributed to the study conception, design, literature search, data acquisition, data analysis, manuscript preparation, and editing. Meanwhile, SS contributed to the study conception, supervising the work, data analysis, manuscript editing, and reviewing and AB contributed to the data analysis and manuscript review.

## CONFLICTS OF INTERESTS

Declared none

## REFERENCES

- Pawar A, Rajalakshmi S, Mehta P, Shaikh K, Bothiraja C. Strategies for formulation development of andrographolide. *RSC Adv.* 2016;6(73):69282-300. doi: 10.1039/C6RA12161F.
- Tan WSD, Liao W, Zhou S, Wong WSF. Is there a future for andrographolide to be an anti-inflammatory drug? Deciphering its major mechanisms of action. *Biochem Pharmacol.* 2017;139:71-81. doi: 10.1016/j.bcp.2017.03.024, PMID 28377280.
- Burgos RA, Hancke JL, Bertoglio JC, Aguirre V, Arriagada S, Calvo M. Efficacy of an andrographis paniculata composition for the relief of rheumatoid arthritis symptoms: a prospective randomized placebo-controlled trial. *Clin Rheumatol.* 2009;28(8):931-46. doi: 10.1007/s10067-009-1180-5, PMID 19408036.
- Li ZZ, Tan JP, Wang LL, Li QH. Andrographolide benefits rheumatoid arthritis via inhibiting MAPK pathways. *Inflammation.* 2017;40(5):1599-605. doi: 10.1007/s10753-017-0600-y, PMID 28584977.
- Yan J, Chen Y, He C, Yang ZZ, Lu C, Chen XS. Andrographolide induces cell cycle arrest and apoptosis in human rheumatoid arthritis fibroblast-like synoviocytes. *Cell Biol Toxicol.* 2012;28(1):47-56. doi: 10.1007/s10565-011-9204-8, PMID 22012578.
- Chellampillai B, Pawar AP. Improved bioavailability of orally administered andrographolide from pH-sensitive nanoparticles. *Eur J Drug Metab Pharmacokinet.* 2011;35(3-4):123-9. doi: 10.1007/s13318-010-0016-7, PMID 21302039.
- Ye L, Wang T, Tang L, Liu W, Yang Z, Zhou J. Poor oral bioavailability of a promising anticancer agent andrographolide is due to extensive metabolism and efflux by P-glycoprotein. *J Pharm Sci.* 2011;100(11):5007-17. doi: 10.1002/jps.22693. PMID 21721007.
- Ramadani AP, Syukri Y, Hasanah E, Syahyeri AW. Acute oral toxicity evaluation of andrographolide self-nanoemulsifying drug delivery system (SNEDDS) formulation. *J Pharm Bioallied Sci.* 2021;13(2):199-204. doi: 10.4103/jpbs.JPBS\_267\_19, PMID 34349480.
- Surini S, Nastiti PD, Putri AR, Putri KSS. Formulation of andrographolide transfersomes gel for transdermal delivery: A preliminary study. *Int J App Pharm.* 2020 March 1;12;Special Issue 1:187-91. doi: 10.22159/ijap.2020.v12s1.FF043.
- Mohammed Magdy I, Makky Amna MA, Abdellatif Menna M. Formulation and characterization of ethosomes bearing vancomycin hydrochloride for transdermal delivery. *Int J Pharm Pharm Sci.* 2014;6(11):190-4.
- Hashimoto N, Nakamichi N, Yamazaki E, Oikawa M, Masuo Y, Schinkel AH. P-Glycoprotein in skin contributes to transdermal absorption of topical corticosteroids. *International Journal of Pharmaceutics.* 2017;521(1-2):365-73. doi: 10.1016/j.ijpharm.2017.02.064.
- Yan N, Tang Z, Xu Y, Li X, Wang Q. Pharmacokinetic study of ferulic acid following transdermal or intragastric administration in rats. *AAPS PharmSciTech.* 2020;21(5):169. doi: 10.1208/s12249-020-01709-w, PMID 32514600.
- Barry BW. Novel mechanisms and devices to enable successful transdermal drug delivery. *Eur J Pharm Sci.* 2001;14(2):101-14. doi: 10.1016/s0928-0987(01)00167-1, PMID 11500256.
- Leonyza A, Surini S. Optimization of sodium deoxycholate-based transfersomes for percutaneous delivery of peptides and proteins. *Int J App Pharm.* 2019;11(5):329-32. doi: 10.22159/ijap.2019v11i5.33615.
- Jalajakshi MN, Chandrakala V, Srinivasan S. An overview: recent development in transdermal drug delivery. *Int J Pharm Pharm Sci.* 2022;14(10):1-9.
- Toutitou E, Dayan N, Bergelson L, Godin B, Eliaz M. Ethosomes-novel vesicular carriers for enhanced delivery: characterization and skin penetration properties. *J Control Release.* 2000;65(3):403-18. doi: 10.1016/s0168-3659(99)00222-9, PMID 10699298.
- Martihandini N, Surini S, Bahtiar A. Andrographolide-loaded ethosomal gel for transdermal application: formulation and *in vitro* penetration study. *Pharm Sci.* 2021;28(3). doi: 10.34172/PS.2021.76.
- Syukri Y, Widarno IS, Adewiyah A, Wibowo A, Martien R, Lukitaningsih E. Development and validation of a simple HPLC-UV method for the quantification of andrographolide in rabbit plasma. *Drug Delivery Technol.* 2017;7(1):22-6.
- Panossian A, Hovhannisyann A, Mamikonyan G, Abrahamian H, Hambardzumyan E, Gabrielian E. Pharmacokinetic and oral bioavailability of andrographolide from Andrographis paniculata fixed combination Kan Jang in rats and human. *Phytomedicine.* 2000;7(5):351-64. doi: 10.1016/S0944-7113(00)80054-9, PMID 11081986.
- Li X, Yuan K, Zhu Q, Lu Q, Jiang H, Zhu M. Andrographolide ameliorates rheumatoid arthritis by regulating the apoptosis-NETosis balance of neutrophils. *Int J Mol Sci.* 2019;20(20). doi: 10.3390/ijms20205035, PMID 31614480.
- Gupta S, Mishra KP, Kumar B, Singh SB, Ganju L. Andrographolide attenuates complete Freund's adjuvant-induced arthritis via suppression of inflammatory mediators and pro-inflammatory cytokines. *J Ethnopharmacol.* 2020;261:113022. doi: 10.1016/j.jep.2020.113022. PMID 32569719.

22. Smit HF, Labadie RP, van Dijk H. Picrorhiza scrophulariiflora, from traditional use to immunomodulatory activity (July); 2000. Available from: <https://dspace.library.uu.nl/bitstream/handle/1874/321/chapter1.pdf>. [Last accessed on 02 Jun 2021].
23. Chourasia MK, Kang L, Chan SY. Nanosized ethosomes bearing ketoprofen for improved transdermal delivery. *Results Pharma Sci.* 2011;1(1):60-7. doi: 10.1016/j.rinphs.2011.10.002, PMID 25755983.
24. Malvern. Zetasizer Nano user manual. Worcestershire, UK: Malvern Instruments limited company; 2013. p. 250.
25. Pathan IB, Jaware BP, Shelke S, Ambekar W. Curcumin loaded ethosomes for transdermal application: Formulation, optimization, *in vitro* and *in vivo* study. *J Drug Deliv Sci Technol.* 2018;44:49-57. doi: 10.1016/j.jddst.2017.11.005.
26. Surini S, Arnedo AR, Iswandana R. Development of ethosome containing bitter melon (*Momordica charantia* Linn.) fruit fraction and *in vitro* skin penetration. *Pharmacogn J.* 2019;11(6):1242-51. doi: 10.5530/pj.2019.11.193.
27. Surini S, Leonyza A, Suh CW. Formulation and *in vitro* penetration study of recombinant human epidermal growth factor-loaded transfersomal emulgel. *Adv Pharm Bull.* 2020;10(4):586-94. doi: 10.34172/apb.2020.070, PMID 33072536.
28. Oktay AN, Ilbasimis Tamer S, Han S, Uludag O, Celebi N. Preparation and *in vitro/in vivo* evaluation of flurbiprofen nanosuspension-based gel for dermal application. *Eur J Pharm Sci.* 2020;155:105548. doi: 10.1016/j.ejps.2020.105548, PMID 32937211.
29. Bast Jr R, Corce C, Hait W, Hong W. *Holland-Frei cancer medicine.* 9<sup>th</sup> ed. 2016. Available from: <http://support.wiley.com>. [Last accessed on 02 May 2021]
30. Katzung BG, Masters SB, Trevor AJ. *Basic and clinical pharmacology.* McGraw-Hill Medical; 2009. p. 1218.
31. Pirvu C, Hlevca C, Ortan A, Prisada R. Elastic vesicles as drug carriers through the skin view project. *Farmacia.* 2010;58(2):128-35.
32. Morsi NM, Aboelwafa AA, Dawoud MHS. Improved bioavailability of timolol maleate via transdermal transfersomal gel: statistical optimization, characterization, and pharmacokinetic assessment. *J Adv Res.* 2016;7(5):691-701. doi: 10.1016/j.jare.2016.07.003, PMID 27660724.
33. Fan J, de Lannoy IAM. Pharmacokinetics. *Biochem Pharmacol.* 2014;87(1):93-120. doi: 10.1016/j.bcp.2013.09.007, PMID 24055064.
34. Sou K. Electrostatics of carboxylated anionic vesicles for improving entrapment capacity. *Chem Phys Lipids.* 2011;164(3):211-5. doi: 10.1016/j.chemphyslip.2011.01.002, PMID 21262210.
35. Padmasri B, Nagaraju R. Formulation and evaluation of novel *in situ* gel system in the management of rheumatoid arthritis. *Int J Appl Pharm.* 2022 Sep 1;14(5):62-8.
36. Patil R, Jain V. Andrographolide: a review of analytical methods. *J Chromatogr Sci.* 2021;59(2):191-203. doi: 10.1093/chromsci/bmaa091, PMID 33221827.
37. Xia YF, Ye BQ, Li YD, Wang JG, He XJ, Lin X. Andrographolide attenuates inflammation by inhibition of NF- $\kappa$ B activation through covalent modification of reduced cysteine 62 of p50. *J Immunol.* 2004;173(6):4207-17. doi: 10.4049/jimmunol.173.6.4207, PMID 15356172.
38. Schinnerling K, Rosas C, Soto L, Thomas R, Aguillon JC. Humanized mouse models of rheumatoid arthritis for studies on immunopathogenesis and preclinical testing of cell-based therapies. *Front Immunol.* 2019;10:203. doi: 10.3389/fimmu.2019.00203, PMID 30837986.
39. Pal R, Chaudhary MJ, Tiwari PC, Nath R, Pant KK. Pharmacological and biochemical studies on protective effects of mangiferin and its interaction with nitric oxide (NO) modulators in adjuvant-induced changes in arthritic parameters, inflammatory, and oxidative biomarkers in rats. *Inflammopharmacology.* 2018;27(2):291-9. doi: 10.1007/s10787-018-0507-8, PMID 29934863.